HSP101/PTEX mediates export of diverse malaria effector proteins into the host erythrocyte

Josh R Beck[1,*], **Vasant Muralidharan**[2,3,*,†], **Anna Oksman**[1,2,3], and **Daniel E Goldberg**[1,2,3]

[1]Department of Molecular Microbiology, Washington University School of Medicine, St. Louis, MO 63110 USA

[2]Department of Medicine, Washington University School of Medicine, St. Louis, MO 63110 USA

[3]Howard Hughes Medical Institute, Washington University School of Medicine, St. Louis, MO 63110 USA

To mediate its survival and virulence the malaria parasite *Plasmodium falciparum* exports hundreds of proteins into the host erythrocyte[1]. In order to enter the host cell, exported proteins must cross the parasitophorous vacuolar membrane (PVM) within which the parasite resides, but the mechanism remains unclear. A putative <u>*Plasmodium* t</u>ranslocon of <u>ex</u>ported proteins (PTEX) has been suggested to be involved for at least one class of exported proteins; however, direct functional evidence for this has been elusive[2–4]. Here we show that export across the PVM requires heat shock protein 101 (HSP101), a ClpB-like AAA+ ATPase component of PTEX. Using a chaperone auto-inhibition strategy, we achieved rapid, reversible ablation of HSP101 function, resulting in a nearly complete block in export with substrates accumulating in the vacuole in both asexual and sexual parasites. Surprisingly, this block extended to all classes of exported proteins, revealing HSP101-dependent translocation across the PVM as a convergent step in the multi-pathway export process. Under export-blocked conditions, association between HSP101 and other components of the PTEX complex was lost indicating that the integrity of the complex is required for efficient protein export. Our results demonstrate an essential and universal role for HSP101 in protein export and provide strong evidence for PTEX function in protein translocation into the host cell.

PTEX is a protein complex found in the PVM, where a translocon responsible for export into the host erythrocyte is expected[2]. The timing of its synthesis is appropriate for a putative translocon and it has a component (EXP2) with weak homology to bacterial hemolysins, which could form a membrane-spanning channel. PTEX contains two additional core components: the novel protein PTEX150 and HSP101, a member of the Clp/HSP100 family of AAA+ ATPases. To directly explore the role of HSP101/PTEX in protein export, we employed a conditional auto-inhibition approach by fusing a DHFR-based destabilization domain (DDD) to the endogenous HSP101 C-terminus (Fig. 1a). While this fusion strategy was originally developed to mediate conditional protein degradation via the proteasome[5,6], we have found that the destabilized tag can conditionally interfere with chaperone function without protein degradation[7]. Following transfection, two independent clones were isolated which had undergone the intended recombination event (Extended Data Fig. 1).

When the DDD-stabilizing small molecule trimethoprim (TMP) was removed from asynchronous HSP101[DDD] cultures, a complete block in growth was observed, with parasites accumulating as late ring-stage forms (Fig. 1b, c). While growth inhibition was TMP concentration dependent, this effect was not a result of HSP101[DDD] degradation (Extended Data Fig. 2a, b). To determine sensitivity to HSP101[DDD] destabilization across the asexual developmental cycle, TMP was removed at regular intervals in synchronized HSP101[DDD] parasites. Removal of TMP in early ring-stages resulted in growth arrest. In contrast, when TMP was removed at or after the beginning of the trophozoite stage (18–24 hours post-invasion), parasite development and re-invasion proceeded normally followed by arrest at the subsequent ring stage (Fig. 1d and Extended Data Fig. 2c, d). Parasite growth was rescued by adding back TMP as late as 48 hours after withdrawal, indicating that arrested ring forms remained viable.

As protein export and PTEX expression also occur in parasite sexual stages, we further evaluated the ability of HSP101[DDD] parasites to form gametocytes required for malaria transmission[8,9]. In gametocytogenesis induction experiments, gametocyte development was severely inhibited when TMP was removed during stage I (Fig. 1e, f and Extended Data Fig. 3). Development was partially rescued by re-introducing TMP after 24 hours. Consistent with PTEX degradation in later gametocyte stages[9], gametocyte formation was largely unaffected by later TMP removal (stage II onwards, 48 and 72 hrs), although a slight delay in development was observed. Collectively, these results demonstrate that HSP101 serves an essential function during asexual and sexual blood-stage development.

To determine the impact of HSP101[DDD] inhibition on protein export, we examined a panel of proteins representative of the diversity of solubility states, targeting motifs, host cell destinations and expression timing observed among the *P. falciparum* repertoire of exported effectors. Most exported proteins contain a pentameric *Plasmodium* export element (PEXEL)[10,11] motif that is cleaved by the aspartic protease plasmepsin V in the parasite ER to license these proteins for export[12,13]. We first examined histidine-rich protein II (HRP2)[14], a soluble PEXEL protein that is exported into the erythrocyte cytosol at the ring stage. To this end, TMP was removed from synchronized HSP101[DDD] schizonts, which were then allowed to develop for 18–24 hours into rings. Remarkably, export of HRP2 into

the host cytosol was completely blocked in nearly all infected RBCs, with the protein accumulating in the parasitophorous vacuole (PV) surrounding the parasite (Fig. 2a, b). Similar results were obtained with the soluble, PEXEL-containing protein REX3[15] and the membrane-associated, PEXEL-containing protein KAHRP[16] (Extended Data Fig. 4a, b and g). Among PEXEL-containing proteins, ring-infected erythrocyte surface antigen (RESA) is uniquely stored in secretory organelles of invading merozoites and discharged into the PV along with PTEX immediately following invasion[3,4,17]. Robust block in RESA export was seen in recently invaded parasites (≤1 hour post invasion), indicating that in the absence of TMP, HSP101[DDD] function is impaired from the time of invasion (Extended Data Fig. 4c, g).

PEXEL-negative exported proteins (PNEPs) are not cleaved by plasmepsin V[18] but appear to contain export signals in their N-termini[19]. As PTEX has thus far been implicated only in translocation of PEXEL proteins[2–4], we examined the PNEP REX1, a protein associated with the cytosolic face of parasite-induced structures in the RBC cytosol called Maurer's clefts, which serve as platforms for sorting of exported proteins[20]. We again observed a block in export with REX1 accumulating in a ring around the parasite where it colocalized with HSP101[DDD] (Fig. 2c and Extended Data Fig. 4g). A similar block was observed for SBP1[21] and REX2[15], integral membrane PNEPs exported to the Maurer's clefts (Extended Data Fig. 4d–g). Export was readily restored when TMP was added back to blocked cultures and restoration was largely insensitive to cycloheximide, indicating that previously synthesized HSP101[DDD] and exported proteins in the PV are sufficient to reactivate export (Extended Data Fig. 5).

As later stages of parasite growth and development are not sensitive to TMP removal (Fig. 1d), we wondered if an export block could be induced after the ring stage. To this end, TMP was removed from synchronous HSP101[DDD] parasites at the late ring stage and export of trophozoite/schizont-specific proteins was assessed 12–24 hours later. We first examined MSRP6, a soluble PNEP peripherally associated with Maurer's clefts[22]. Parasites lacking TMP displayed a dramatic block of MSRP6 export while SBP1, exported before the block, was found in the erythrocyte (Fig. 2d and Extended Data Fig. 4g). Similar results were seen for the PNEP PfEMP1, a variable surface antigen and key virulence determinant for *P. falciparum* malaria[23] (Fig. 2e and Extended Data Fig. 4g). Importantly, PfEMP1 trafficking to the RBC surface is dependent on several additional exported proteins[1]. Thus, while these results indicate delivery of PfEMP1 to the RBC surface is HSP101-dependent, we cannot exclude the possibility that this block is an indirect result of a failure to export other proteins required for PfEMP1 trafficking rather than a direct effect of HSP101 inactivation. Finally, we examined PFA660, a PEXEL-containing HSP40 found in parasite-induced membrane structures in the RBC called J-dots[24]. Again, washout of TMP efficiently blocked export as visualized by expression of a PFA660-GFP fusion protein in live parasites (Fig. 2f and Extended Data Fig. 4g). Together, these data show that HSP101 function is necessary for export but not parasite development in the trophozoite and schizont stages.

Formation of a normal digestive vacuole containing hemozoin (Fig. 2d–f, DIC panels) indicates that hemoglobin uptake and degradation proceeded normally in these parasites, a process requiring proteases that are secreted into the PV before entering the digestive

vacuole where they are activated[25]. Indeed, maturation of plasmepsin II was unaffected by TMP removal, indicating normal trafficking through the PV to the digestive vacuole (Extended Data Fig. 6). Additionally, HSP101 inactivation did not affect egress, a process mediated by secretion of the PfSUB1 protease into the PV[26]. Since PV processes unrelated to export proceed normally when HSP101 function is interrupted, HSP101 appears to serve a specific role in export. Furthermore, parasites expressing a PV-targeted GFP[DDD] fusion protein showed no defect in growth or export, indicating the HSP101[DDD] phenotype is not an indirect result of destabilizing the DDD in the PV compartment (Extended Data Fig. 7).

Finally, we examined PfGECO, a PEXEL-containing HSP40 that is specifically expressed in gametocytes[27]. Again, export of PfGECO across the PVM was dramatically blocked in stage I gametocytes, showing an HSP101 requirement for protein export in sexual stages (Extended Data Fig. 4h).

Parasite nutrient acquisition is supported by establishment of a *Plasmodium* surface anion channel (PSAC or new permeability pathways) at the late ring stage. This channel modifies the sensitivity of the infected RBC to osmotic lysis upon solute uptake. Following TMP removal prior to RBC invasion, arrested ring-stage HSP101[DDD] parasites failed to lyse in the presence of sorbitol (Fig. 3a). In contrast, sensitivity to osmotic lysis developed normally when TMP was removed at the end of the ring stage (Fig. 3b). CLAG3 proteins localize to the infected RBC periphery and are the only parasite proteins known to be involved in PSAC activation[28]. Interestingly, we observed no change in CLAG3 localization to the host periphery when export was blocked, suggesting that additional exported factors are required to activate PSAC (Fig. 3c). CLAG3 may be directly secreted into the RBC membrane during invasion similar to other rhoptry proteins[29], or could traffic from the PV by an HSP101-independent export pathway. Nutrient uptake via PSAC is an essential process and block of its formation at the late ring stage may be the lethal event that follows HSP101 inhibition.

We reasoned that export block might arise from the disordered DDD interfering with interactions between HSP101[DDD] and other PTEX components. To test this, HSP101[DDD] was immunoprecipitated (IP) from parasite lysates. Remarkably, while localization of HSP101[DDD] and EXP2 was unchanged +/− TMP (Extended Data Fig. 8a–c), their interaction decreased by more than 90% in the absence of TMP (Fig. 4a, f). A similar loss of HSP101-EXP2 interaction (70% decrease) was observed in reciprocal IP experiments (Fig. 4b, f). In contrast, association of HSP101[DDD] with RESA increased by more than two-fold (Fig. 4c, f and Extended Data Fig. 9a). To analyze PTEX150 interactions, we generated an HSP101[DDD] strain expressing a second copy of PTEX150 with a FLAG tag. The fusion protein localized to the PVM and distribution was unchanged +/− TMP (Extended Data Fig. 8d, e). Interaction between HSP101[DDD] and PTEX150 was substantially decreased in the absence of TMP (84% decrease, Fig. 4d, f) while interactions between PTEX150 and EXP2 were not affected (Fig. 4e, f and Extended Data Fig. 9b). We conclude that destabilization of the DHFR-domain fold results in HSP101[DDD] dissociation from the PTEX complex, producing a block in translocation of exported proteins out of the PV (Fig. 4g). Increased association with RESA under these conditions shows that interaction with exported substrates is not impaired. Interestingly, we also observed increased interaction between EXP2 and RESA in the absence of TMP (Fig. 4c, f and Extended Data Fig. 9a), suggesting

that PTEX components can interact with substrates independent of HSP101 but that HSP101 is needed to drive export, likely through substrate unfolding and/or translocation (although we cannot exclude the possibility that association of RESA and HSP101[DDD] in the absence of TMP results from "stickiness" of the destabilized DDD).

These data demonstrate that HSP101 is required to mediate protein export in *P. falciparum*. As HSP101 is a major component of PTEX, our results provide strong functional evidence for a PTEX role in protein translocation (Fig. 4g), though we cannot formally rule out the possibility that these proteins perform some other critical activity upstream of actual translocation across the PVM. The essential role of HSP101 in parasite survival and export of key virulence determinants provides impetus for pursuing PTEX as a drug target.

Full Methods

Cell Fractionation

TMP was removed from synchronous 13F10 parasites at the late schizont stage and development was allowed to proceed +/− 10 μM TMP for 18 hours to the ring stage. Ring-stage parasites were enriched to >95% parasitemia by an initial tetanolysin treatment of 2.5 hemolytic units (HU) for 20 minutes as described[30]. Samples were then fractionated by sequential treatment with tetanolysin (1 HU for 20 min) and saponin (0.035% for 5 min) as described[19,30].

Parasite strains, culture and genetic modification

Parasite culture and flow cytometry analysis was performed as described[7]. Cloning was performed using the In-Fusion system (Clontech) unless otherwise noted. For generation of HSP101[DDD] parasites, the DDD cassette was PCR amplified from plasmid pGDB[6] with primers 5′-GAGCAGCTGACCTAGGTACCCATACGATGTTCCAGATTACGCTTACCCATACGATGTTCCAGATTACGCTTACCCATACGATGTTCCAGATTACGCTATCAGTCTGATTGCGGCGTTAGCGGTAGATCACGTTATCGGC-3′ and 5′-TAACTCGACGCGGCCGTCATCGCCGCTCCAGAATCTCAAAGCAATAGCTGTGAGAG-3′ to incorporate a 5′ 3xHA tag. The amplicon was inserted into plasmid pPM2GT[25] between restriction sites *AvrII/EagI*. The BSD cassette was then PCR amplified from pGDB with primers 5′-ATGCCTGCAGGTCGATTGCATGCTTAGCTAATTCGCTTG-3′ and 5′-GAGAAATCTAGAGGTACCGAGCTCGATCTGCCGGTCTCC-3′ and inserted between restriction sites *SalI/BglII*. Finally, a portion of the 3′ genomic locus of HSP101 up to but not including the stop codon was PCR amplified from *P. falciparum* genomic DNA using primers 5′-ACGATTTTTTCTCGAGCGAAAACTTTTATGGTATTAATATAACAGATAAAGCTTTAGTAGCAGCAGC-3′ and 5′-CTGCACCTGGCCTAGGGGTCTTAGATAAGTTTATAACCAAGTTTTTAGCTTTACTATTATAATCAACAAATACATCC-3′ and inserted between restriction sites *XhoI/AvrII*. The resulting plasmid pHSP101-HDB was transfected into the 3D7-derived parental strain PM1KO[31], which contains an hDHFR expression cassette conferring resistance to TMP. Selection, cycling and cloning were performed as described[7]. TMP was maintained in the

medium throughout. Two clones from independent transfections were isolated and designated 13F10 and 14G11. Integration was detected by PCR using the primers 5′-CCTCCTTCAGTAGATATGACCG-3′ and 5′-CTAACGCCGCAATCAGACTG-3′ and confirmed by Southern blot using a probe to the 3′ end of the HSP101 gene, generated with the primers 5′-CGAAAACTTTTATGGTATTAATATAACAG-3′ and 5′-GGTCTTAGATAAGTTTATAACCAAG-3′.

For gene expression, the episomal expression plasmid pyEOE[7] containing a yeast dihydroorotate dehydrogenase selection cassette was modified for transposase-mediated genomic integration by inserting a *piggyBac* element containing inverted terminal repeats amplified from plasmid pXL-BACII-DHFR[32] with primers 5′-GGAATTTCCTTATAAGATCTTAATACGACTCACTATAGGGCGAATTGGG-3′ and 5′-ATAATGGTTTCTTAGACGTCGATAAAAGTTTTGTTACTTTATAGAAGAAATTTTGAG-3′ between the restriction sites *BglII/AatII*, resulting in the plasmid pTyEOE. For expression of PFA660-GFP, the PFA660 coding sequence was PCR amplified from parasite cDNA with primers 5′-ACGATTTTTTCTCGAGATGGCAACCTTAAGGAAAAGC-3′ and 5′-CTGCACCTGGCCTAGGATAACTCTCTTTAAATATCTCTTTTATC-3′ and inserted into plasmid pTyEOE between restriction sites *XhoI/AvrII*, placing the gene under the control of the HSP86 promoter and generating a C-terminal GFP fusion. For expression of the PV-targeted GFP-DDD fusion protein, sequence encoding GFP fused to DDD with a C-terminal HA tag was amplified from plasmid pGDB with the forward primer 5′-ACCCCGGGATCTCGAGATGACAAGAAGATATTTAAAGTATTATATTTTTGTTACTTTATTGTTTTTTTGTTCAAGTTATTAATAATGTATTGTGTGCTCCTAGGGCAGCAAGTAAAGGAGAAGAACTTTTCACTGGAG-3′ (encoding the HSP101 signal peptide, amino acids 1-27) and the reverse primer 5′-AACTCGACGCGGCCGTCAAGCGTAATCTGGAACATCGTATGGG-3′. This amplicon was inserted in plasmid pTyEOE between the restriction sites *XhoI/EagI*. For expression of the PTEX150-FLAG fusion protein, sequence encoding a 6xFLAG epitope was generated with the primer 5′-TTGATAGACCTAGGGACTACAAGGACGACGACGACAAGGATTATAAAGATGATGATGATAAAGATTATAAAGATGATGATGATAAAGATTATAAAGATGATGATGATAAAGATTATAAAGATGATGATGATAAAGATTATAAAGATGATGATGATAAAT AACGGCCGCGTCGAGTT-3′ and its reverse complement. The primers were annealed and inserted between restriction sites *AvrII/EagI* in plasmid pTyEOE, resulting in plasmid pTyEOE-6xFLAG. The PTEX150 gene (which contains no introns) was then PCR amplified from parasite genomic DNA with its endogenous 5′ UTR up to but not including the stop codon using primers 5′-GATCGAGACGTCCTCTTTGTGGTCAAAATAAGTAAAATTTTATAAATTC-3′ and 5′-GTCACCTAGGATTGTCGTCCTCTTCTTCGTCC-3′ and inserted between restriction sites *AatII/AvrII* by standard ligation. pTyEOE-derived plasmids were co-transfected with plasmid pHTH for transient expression of the *piggyBac* transposase to mediate genomic integration[32].

Growth assays

For asynchronous growth assays, parasites were subcultured 1:2 each day to avoid confounding effects from high parasite density in making growth rate comparisons between different samples. Parasitemia at each time points was back calculated based on the subculturing schedule. Data were fit to exponential growth equations using Prism (Graphpad Software, Inc.). In synchronous growth assays, daily media changes were performed without subculture. Parasitemia was determined by flow cytometry.

Gametocyte induction

Synchronous 13F10 parasites at 5–7% parasitemia were stressed by increasing hematocrit to 4% at the mid-trophozoite stage for ~12 hours. Hematocrit was returned to 2% at the schizont stage and TMP washout was performed at late schizont stage shortly before rupture and at 24 hr intervals thereafter. Asexual parasites were killed by treatment with 50 mM N-acetylglucosamine in the following cycle.

Antibodies

The following antibodies were used for IFA and Western blot: rabbit polyclonal anti-HA (Life Technologies) (IFA: 1:100); rabbit polyclonal anti-HA (Sigma) (WB 1:1000); rat anti-HA mAb clone 3F10 (Roche) (IFA: 1:100, WB: 1:1000); mouse anti-FLAG mAb clone M2 (Sigma) (IFA: 1:100, WB 1:500); mouse anti-EXP2 mAb clone 7.7[33] (IFA: 1:1000, WB: 1:1000); mouse anti-HRP2 mAb 2G12[14] (IFA 1:1000, WB: 1:500); mouse anti-RESA mAb clone 28/2[34] (IFA: 1:1000, WB: 1:1000); rabbit polyclonal anti-BiP[35] (WB: 1:1000); rabbit polyclonal anti-REX1[36] (IFA: 1:1000); mouse polyclonal anti-REX2[15] (IFA: 1:500); mouse polyclonal anti-REX3[15] (IFA: 1:500); rabbit polyclonal anti-SBP1[21] (IFA: 1:500); mouse polyclonal anti-MSRP6[22] (IFA: 1:500); mouse polyclonal anti-PfGECO[27] (IFA: 1:300); rabbit polyclonal anti-Pfs16[37] (IFA: 1:500); rabbit polyclonal anti-PfEMP1 ATS[38] (IFA: 1:200); mouse polyclonal anti-CLAG3[28] (IFA: 1:300); rabbit polyclonal anti-PM2 antibody 737[39] (WB 1:2000); rabbit polyclonal anti-KAHRP[16] (IFA: 1:500); rabbit polyclonal anti-SERP[40] (IFA: 1:500, WB: 1:1000).

Light microscopy and image processing

For indirect IFA detecting HRP2, REX3, PfGECO and Pfs16, cells were allowed to settle on coverslips coated with concanavalin A and fixed with a mixture of 4% paraformaldehyde and 0.0075% glutaraldehyde in PBS. For indirect IFA detecting HA and FLAG epitopes, EXP2, RESA, REX1, REX2, SBP1, MSRP6, PfEMP1, and KAHRP, thin smears were air dried and fixed with room temperature acetone. For indirect IFA detecting CLAG3 and SBP1, thin smears were air dried and fixed with ice-cold 90% acetone/10% methanol. Primary antibodies were detected by Alexa Fluor 488 or 594 secondary IgG antibodies (Life Technologies) used at 1:2000. Image stacks were collected at z-increments of 0.2 μm with an ORCA-ER CCD camera (Hamamatsu) and AxioVision software on an Axio Imager.M1 microscope (Zeiss) using a 100x oil immersion objective. Deconvolved images were generated using manufacturer specified point-spread functions and displayed as maximum intensity projections. Adjustments to brightness and contrast were made for display

purposes. Live imaging was performed as previously described[41]. All IFA and live imaging experiments were repeated at least twice.

Immuno electron microscopy

For immunolocalization at the ultrastructural level, infected RBCs were fixed in 4% paraformaldehyde/0.05% glutaraldehyde (Polysciences Inc.) in 100mM PIPES/0.5mM MgCl2, pH 7.2 for 1 hour at 4°C. Samples were then embedded in 10% gelatin and infiltrated overnight with 2.3M sucrose/20% polyvinyl pyrrolidone in PIPES/MgCl2 at 4°C. Samples were trimmed, frozen in liquid nitrogen, and sectioned with a Leica Ultracut UCT cryo-ultramicrotome (Leica Microsystems Inc.). 50 nm sections were blocked with 5% fetal bovine serum/5% normal goat serum for 30 min and subsequently incubated with primary antibodies followed by secondary anti-rabbit conjugated to 18 nm colloidal gold (Jackson ImmunoResearch Laboratories, Inc.). Sections were washed in PIPES buffer followed by a water rinse, and stained with 0.3% uranyl acetate/2% methyl cellulose. Samples were viewed with a JEOL 1200EX transmission electron microscope (JEOL USA Inc.) equipped with an AMT 8 megapixel digital camera (Advanced Microscopy Techniques). All labeling experiments were conducted in parallel with controls omitting the primary antibody. These controls were consistently negative at the concentration of colloidal gold conjugated secondary antibodies used in these studies.

Assessment of export in recently invaded parasites

To monitor RESA export immediately after invasion, synchronous late schizonts were purified over Percoll and then mixed with fresh RBCs in pre-warmed media. Cultures were shaken at 37° C for one hour. After lysis of unruptured schizonts by sorbitol treatment, samples were fixed for IFA and stained with RESA antibodies as described above.

Osmotic Lysis assays

Osmotic lysis assays were performed as described by incubating cells in 290 mM D-sorbitol and measuring hemoglobin release by absorbance at 405 nm[42,43]. Samples were prepared as follows: TMP was removed or not from synchronous, late schizont-stage 13F10 parasites and development was allowed to proceed for 24 hours, resulting in 25% parasitemia cultures of early trophozoites (+TMP) or arrested late ring-forms (−TMP). Alternatively, TMP was removed or not from synchronous 13F10 parasites at the late ring-stage and development was allowed to proceed 24 hours before magnet purification to >95% parasitemia. In either case, the final concentration of cells in each sample was 1×10^8/ml. At the end of the assay, samples were lysed with saponin and data were normalized to these values (100% lysis).

Immunoprecipitation

For immunoprecipitation, TMP was removed or not from synchronous parasites at the early trophozoite-stage and parasites were allowed to develop for 24 hours to late schizonts and early rings. Parasites were then harvested with 0.035% saponin in PBS and lysed in 0.5% triton X-100 in PBS. Following sonication, lysates were cleared by centrifugation at 16,000 × g for 5 min and supernatants were nutated for 3 hours at 4°C with indicated antibodies and dynabeads coupled to protein G or protein A (or dynabeads alone as a negative control when

necessary) (Life Technologies). Immune complexes were purified on magnets with extensive washing with 0.5% triton X-100 in PBS and then lysed in sample buffer.

Western blots

Western blot analysis was performed using an Odyssey infrared imaging system (LI-COR Biosciences). Primary antibodies were detected by IRDye 680 and 800-conjugated secondary antibodies (LI-COR Biosciences) used at 1:15,000. Quantitative measurements were made with Image Studio software (LI-COR Biosciences).
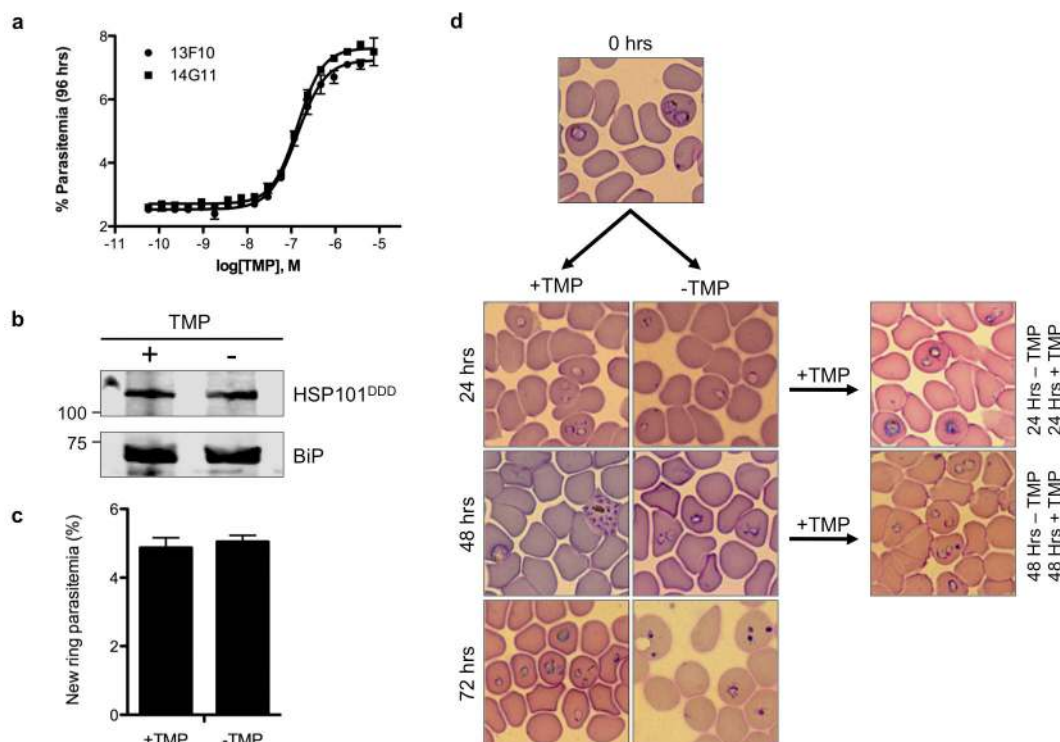
Extended Data
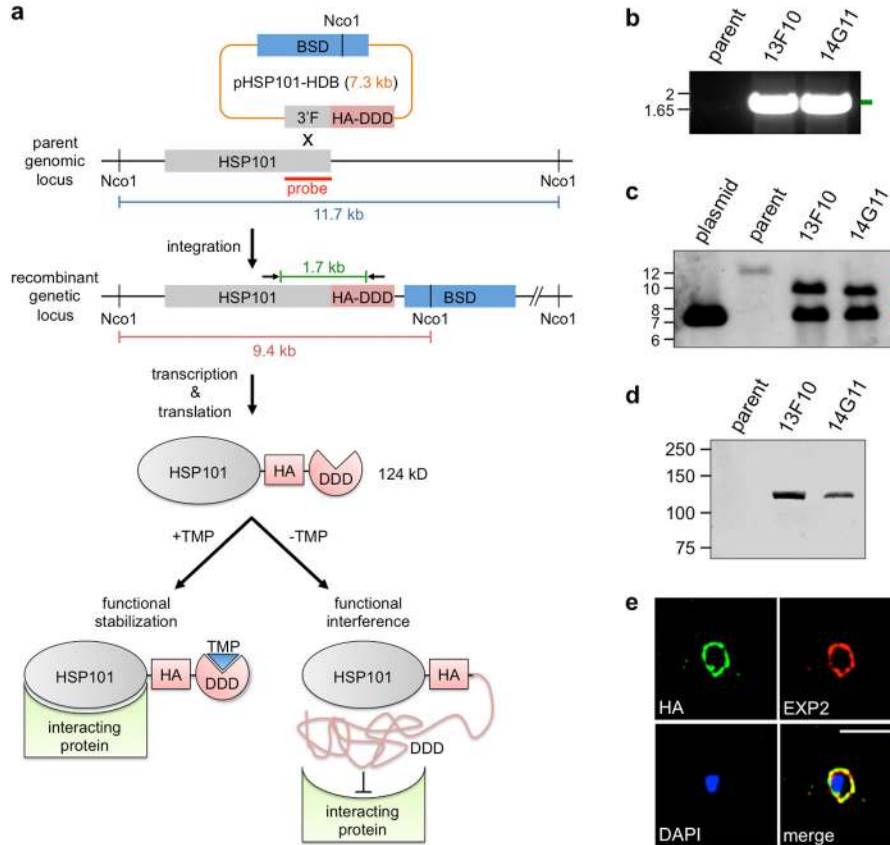
Extended Data Figure 1. Generation of HSP101^{DDD} strains
a, Schematic of strategy to generate HSP101^{DDD} parasites. 3′F, 3′ flank for homologous recombination; BSD, blasticidin S deaminase; TMP, trimethoprim; HA, hemagglutinin tag; DDD, DHFR destabilization domain. **b,** Diagnostic PCR showing integration of the DDD fusion in the two independent clones 13F10 and 14G11. Primers shown as black arrows in **a**. Image is representative of two independent experiments. **c,** Southern blot showing integration of plasmid pHSP101-HDB occurred at the intended genomic locus. Expected *NcoI* digestion products and sizes are indicated in blue, red and orange in **a**. The 7.3 kb band in 13F10 and 14G11 indicates the presence of concatamers commonly observed in *P. falciparum*. Image is representative of one experiment. **d,** Western blot with anti-HA antibodies detects a 124 kD band in clones 13F10 and 14G11. Image is representative of two

independent experiments. **e,** IFA of acetone-fixed 13F10 parasites showing colocalization of HSP101^DDD and EXP2 at the PVM. Scale bar = 5μm. Images are representative of two independent experiments.

Extended Data Figure 2. Characterization of HSP101^DDD strains
a, TMP dose-response for 13F10 and 14G11 parasites grown for 96 hours was measured. Error bars represent s. d. of three technical replicates. **b,** Western blot on lysates from asynchronous 13F10 parasites grown +/− TMP for 24 hours. BiP serves as a loading control. Blotting with anti-HA antibody shows no decrease in HSP101^DDD protein levels relative to the BiP loading control. Images are representative of two independent experiments. **c,** Quantification of new ring parasitemia +/− TMP. In a parallel experiment to that shown in Fig 1d (but beginning with lower parasitemia cultures), new rings were counted in Giemsa-stained smears of synchronous 13F10 parasites where TMP was removed or not during the proceeding trophozoite stage. No significant difference in the resulting new ring parasitemia was observed +/− TMP, indicating no difference in re-invasion efficiency -TMP. Error bars represent s. d. of three technical replicates. Data are representative of two independent experiments. **d,** Giemsa-stained smears of synchronous 13F10 parasites grown +/− TMP from Fig. 1d. Reintroduction of TMP after 24 or 48 hours restored progression through the intraerythrocytic cycle. After 72 hours without TMP, most parasites appeared as dead, pyknotic forms. Images are representative of three independent experiments.
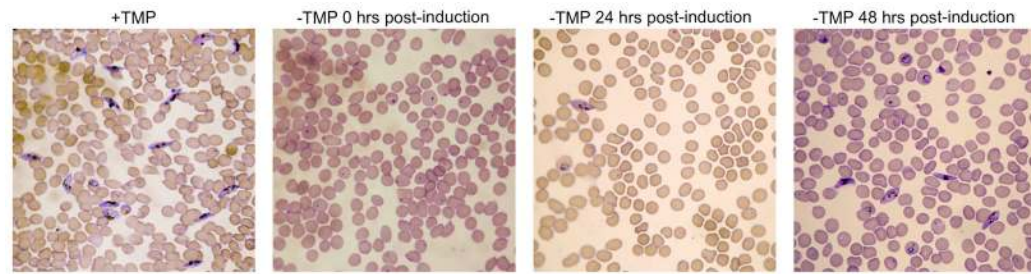
Extended Data Figure 3. HSP101 function is critical for early stage gametocyte development
Giemsa-stained smears from day nine post gametocyte induction as quantified in Fig. 1e.
TMP was removed from parallel samples at 24-hour intervals beginning just prior to
reinvasion (0 hrs) following gametocytogenesis induction. Data are representative of 4
independent experiments. While control (+TMP) gametocytemia varied between
experiments, a similar effect on gametocyte formation was observed in each experiment
following TMP removal.
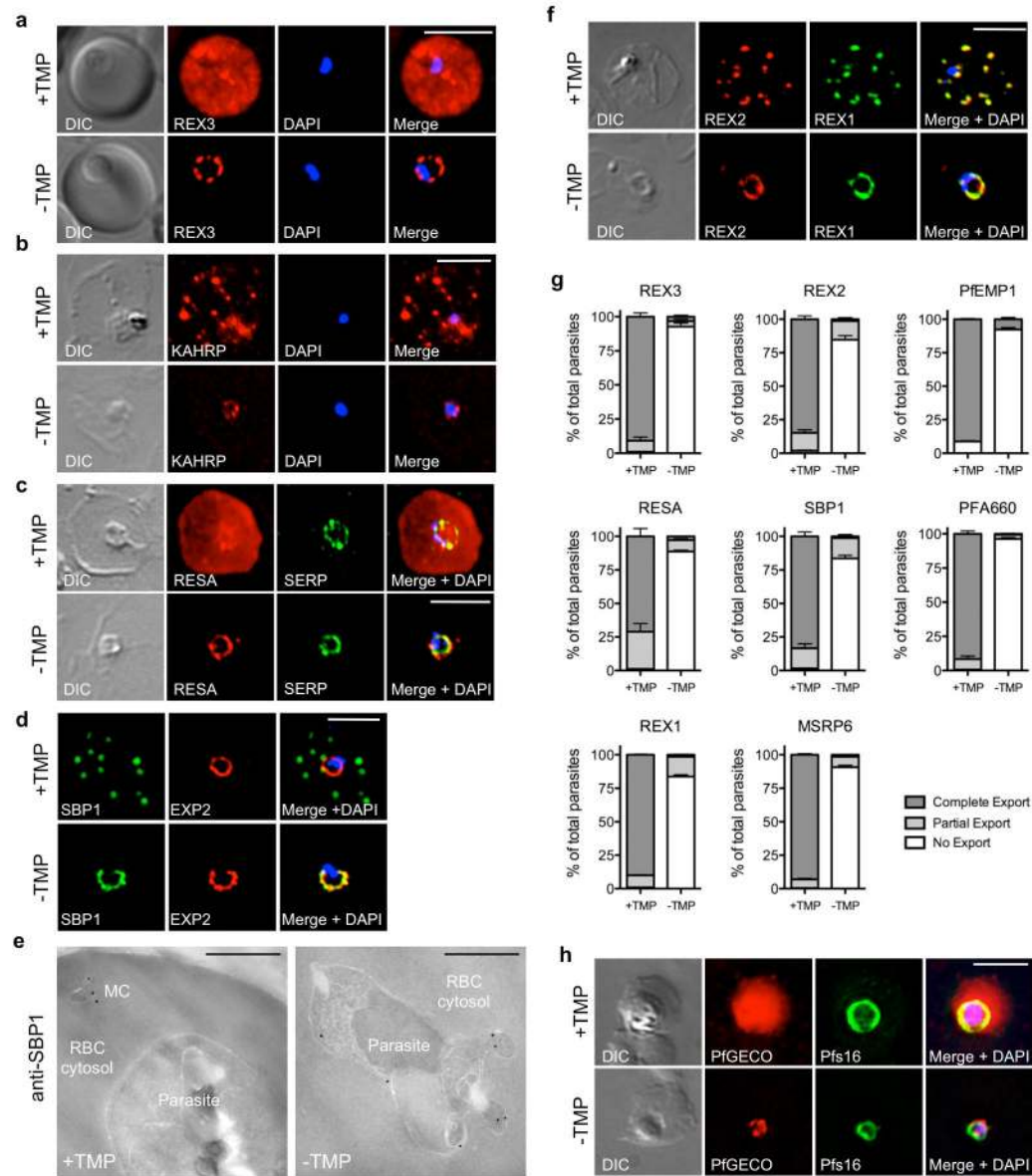
Extended Data Figure 4. Localization and quantification of exported proteins following HSP101^{DDD} inactivation

a–f, IFA and immuno electron microscopy (EM) of ring-stage 13F10 parasites +/− TMP. TMP was removed in late schizont stage and parasites were allowed to reinvade and grow 18–24 hours before fixation with paraformaldehyde (a) or acetone (b–d, f). Immuno EM fixation (e) is detailed in methods. A similar export block with accumulation of the exported protein at the parasite periphery was observed in each case when TMP was removed. The soluble PEXEL-containing protein REX3 (a) is normally exported into the host RBC cytosol. The PEXEL-containing KAHRP protein (b) is normally exported through Maurer's clefts to knob structures at the cytoplasmic face of the infected RBC membrane. The PEXEL-containing protein RESA (c) is normally exported to the RBC periphery. SERP is a marker for the PV. SBP1 (d) is an integral membrane PNEP normally exported to the Maurer's clefts. In the absence of TMP, blocked SBP1 colocalizes with EXP2. **e,** Immuno

electron microscopy showing localization of SBP1 in ring-stage parasites +/− TMP. MC, Maurer's cleft. Scale bars = 500nm. Images are representative of one experiment. REX2 (f) is an integral membrane PNEP normally exported to the Maurer's clefts. **g,** Quantification of export block by IFA for exported proteins shown here and in Fig. 2c–f. Export was scored as complete (all signal in the host cell), partial (signal within the host cell but also within the PV) or no export (signal only seen within the PV and not in the host cell). Example images of each scoring scenario are given for REX1 in Extended Data Fig. 5a. In the case of PfEMP1, cells were scored as having PfEMP1 signal at the RBC periphery (complete export) or not (no export) due to the fact that some PfEMP1 signal is always seen within the PV under normal export conditions (see Fig. 2e, +TMP). Error bars represent s. d. of three technical replicates. Data are representative of at least two independent experiments. **h,** IFA of PfGECO in paraformaldehyde-fixed, stage I gametocytes 36 hours post invasion +/− TMP. Pfs16 is a gametocyte-specific PVM marker. All IFA scale bars = 5μm. All IFA images (a–d, f, h) are representative of two independent experiments.
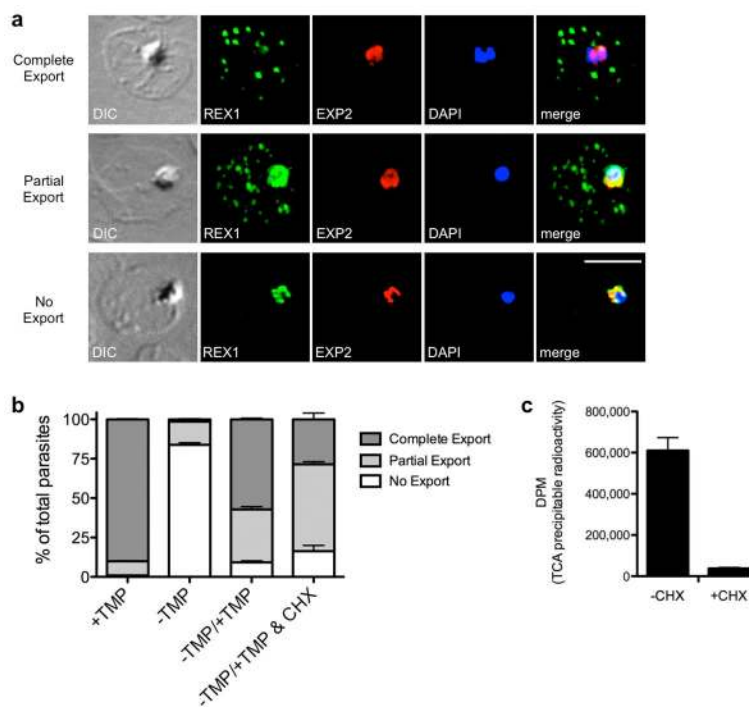
Extended Data Figure 5. Reactivation of export does not require new protein synthesis
a–b, TMP was removed in late schizonts and parasites were allowed to reinvade and develop for 18 hours before TMP add back with or without 10 μg/ml cycloheximide (CHX). Parasites were acetone-fixed 24 hours later and processed for IFA. Export was scored as complete (no REX1 retained within the EXP2-labeled PVM), partial (REX1 in the host cell and retained within the PVM) or no export (no REX1 signal beyond the PVM). Error bars represent s. d. of three technical replicates. Data are representative of two independent experiments. Scale bar = 5μm. **c,** Metabolic labeling with [^{35}S]methionine/cysteine, performed as previously described[44], confirms that CHX treatment conditions inhibit new protein synthesis. Parasite proteins were TCA-precipitated and incorporated radioactivity

was determined through scintillation counting. Error bars represent s. d. of three technical replicates.
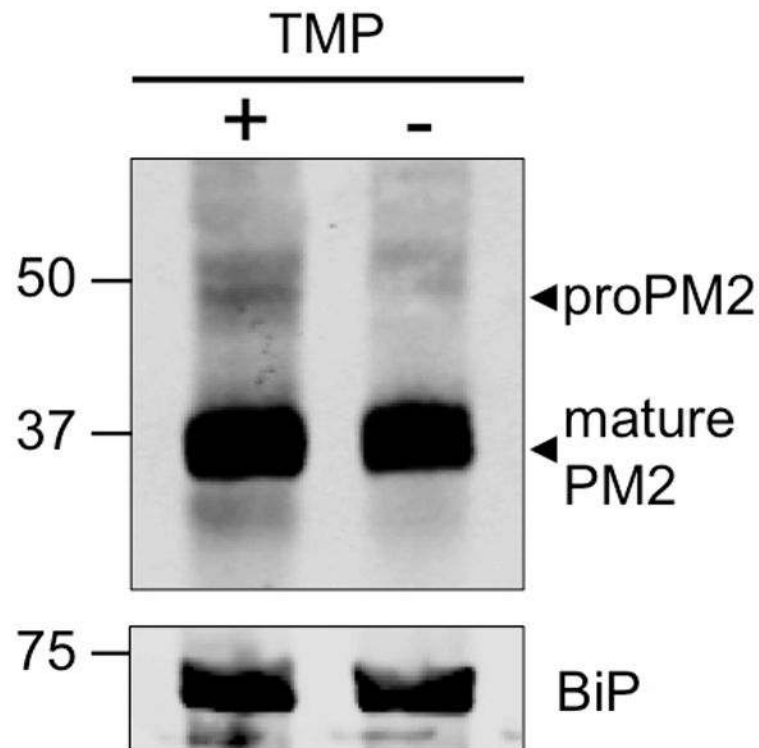

Extended Data Figure 6. Maturation of plasmepsin 2 is not impacted by inactivation of HSP101
Western blot showing normal maturation of plasmepsin 2 (PM2) in asynchronous parasites after 24 hours −TMP. BiP serves as a loading control. Maturation requires proPM2 trafficking through the PV prior to internalization to the digestive vacuole where maturation occurs[25]. Images are representative of two independent experiments.
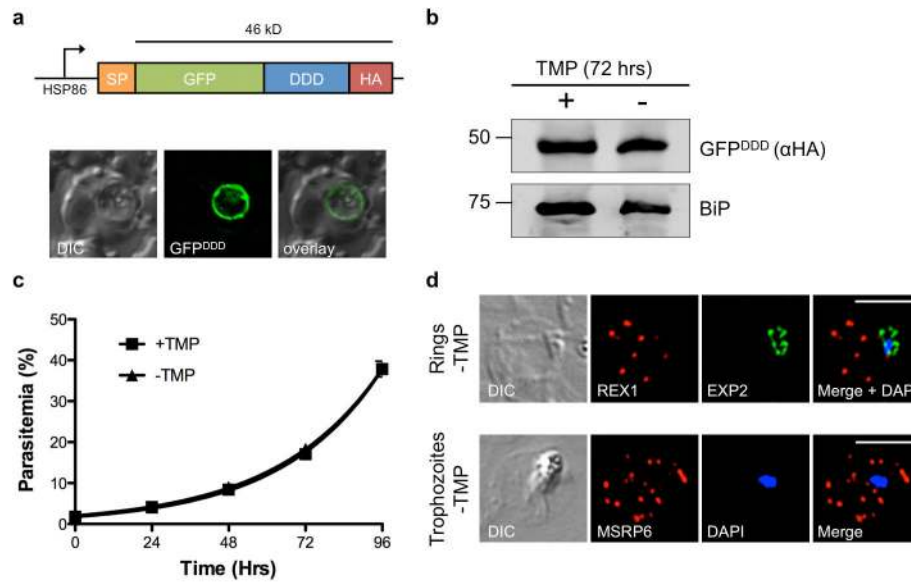
Extended Data Figure 7. DDD targeted to the PV independent of HSP101 does not interfere with parasite growth or export

a, Schematic of the PV-targeted GFP-DDD fusion protein consisting of a signal peptide appended to a GFP-DDD fusion with a C-terminal HA epitope tag and expressed under the control of the HSP86 promoter. The predicted size of the fusion protein after signal peptide cleavage is 46 kD. Live imaging of GFP demonstrates PV targeting of the fusion protein. Images are representative of two independent experiments. **b,** Western blot showing GFP^{DDD} is not degraded in the absence of TMP. Synchronized GFP^{DDD} parasites were grown 72 hours with or without TMP before purification over Percoll and treatment with tetanolysin to release the RBC cytosol but not the PV contents. The GFP^{DDD} fusion was detected with anti-HA antibodies. BiP serves as a loading control. Images represent one experiment. **c,** Growth analysis of asynchronous GFP^{DDD} parasites shows no growth defect -TMP. Error bars represent s. d. of three technical replicates. Data are representative of two independent experiments. **d,** IFA showing no defect in export in GFP^{DDD} parasites in the absence of TMP. No difference was observed in export of ring-specific (REX1) and the trophozoite-specific (MSRP6) exported proteins in the presence or absence of TMP. All scale bars = 5μm. Images represent one experiment.
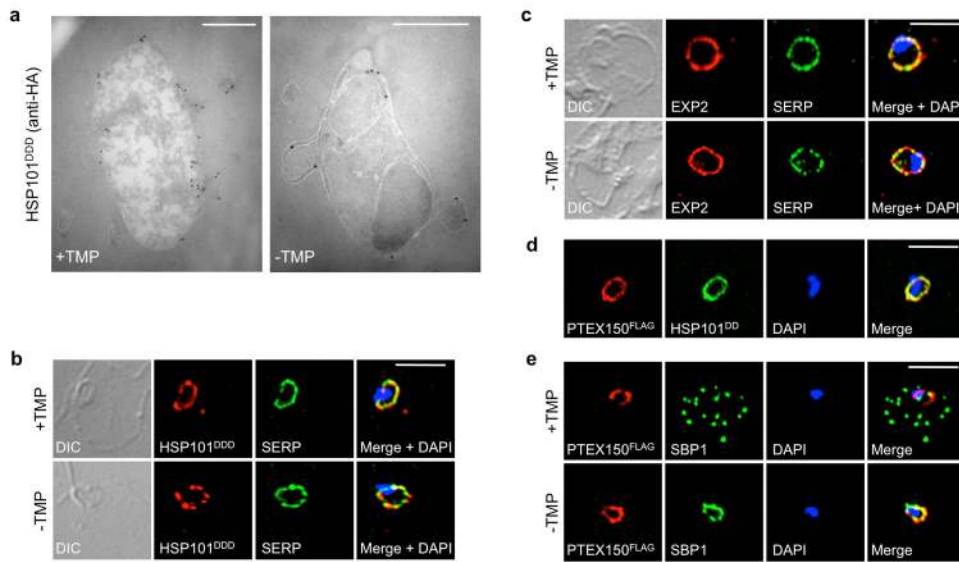
Extended Data Figure 8. Localization of PTEX components is unchanged under export blocking conditions

a, Immuno EM showing localization of HSP101^{DDD} in ring-stage parasites +/− TMP. TMP was removed or not from synchronous late schizonts and parasites were allowed to re-invade and develop for 18 hours prior to fixation. Scale bars = 500nm. Images represent one experiment. **b, c,** IFA of 13F10 parasites showing co-localization between HSP101^{DDD} or EXP2 and the PV marker SERP +/− TMP, indicating localization of these PTEX components is not altered under export blocking conditions. TMP TMP treatment was performed as in **a** prior to fixation with acetone and processing for IFA. **d, e,** IFA of ring-stage 13F10 parasites expressing a PTEX150-FLAG fusion. The upper panel (d) shows co-localization with HSP101^{DDD}. The lower two panels (e) show PTEX150 remains at the PVM during export block and partially colocalizes with blocked SBP1. TMP treatment and fixation as in **b,c**. All IFA scale bars = 5μm. All IFA images (b–e) are representative of two independent experiments.
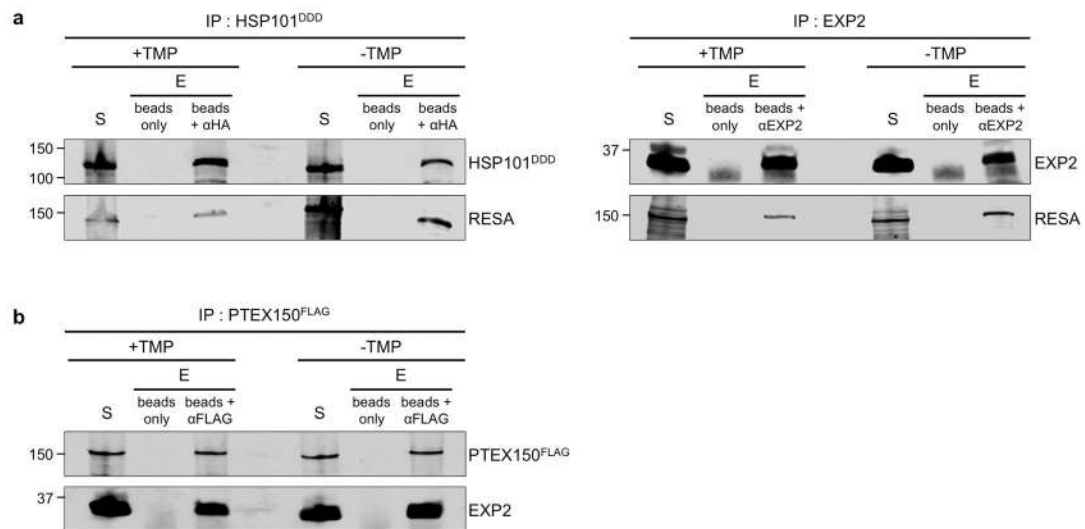
Extended Data Figure 9. Immunoprecipitation bead controls indicate target-specific interactions
Replicate IP experiments to those shown in Fig. 4c, e with bead controls included. Purification of (a) RESA by HSP101^{DDD} or EXP2 and purification of (b) EXP2 by PTEX150^{FLAG} is specific to the target antibodies. IP experiments were performed in parallel by incubating equivalent portions of lysate supernatant input with beads alone or beads and the indicated IP antibodies. S, supernatant input. E, elution. Data are representative of two independent experiments.

Acknowledgments

References

1. Boddey JA, Cowman AF. Plasmodium nesting: remaking the erythrocyte from the inside out. Annu Rev Microbiol. 2013; 67:243–269. [PubMed: 23808341]

2. de Koning-Ward TF, et al. A newly discovered protein export machine in malaria parasites. Nature. 2009; 459:945–949. [PubMed: 19536257]

3. Bullen HE, et al. Biosynthesis, localization, and macromolecular arrangement of the Plasmodium falciparum translocon of exported proteins (PTEX). J Biol Chem. 2012; 287:7871–7884. [PubMed: 22253438]

4. Riglar DT, et al. Spatial association with PTEX complexes defines regions for effector export into Plasmodium falciparum-infected erythrocytes. Nat Commun. 2013; 4:1415. [PubMed: 23361006]

5. Iwamoto M, Bjorklund T, Lundberg C, Kirik D, Wandless TJ. A general chemical method to regulate protein stability in the mammalian central nervous system. Chem Biol. 2010; 17:981–988. [PubMed: 20851347]

6. Muralidharan V, Oksman A, Iwamoto M, Wandless TJ, Goldberg DE. Asparagine repeat function in a Plasmodium falciparum protein assessed via a regulatable fluorescent affinity tag. Proc Natl Acad Sci U S A. 2011; 108:4411–4416. [PubMed: 21368162]

7. Muralidharan V, Oksman A, Pal P, Lindquist S, Goldberg DE. Plasmodium falciparum heat shock protein 110 stabilizes the asparagine repeat-rich parasite proteome during malarial fevers. Nat Commun. 2012; 3:1310. [PubMed: 23250440]

8. Silvestrini F, et al. Protein export marks the early phase of gametocytogenesis of the human malaria parasite Plasmodium falciparum. Mol Cell Proteomics. 2010; 9:1437–1448. [PubMed: 20332084]

9. Matthews K, et al. The Plasmodium translocon of exported proteins (PTEX) component thioredoxin-2 is important for maintaining normal blood-stage growth. Mol Microbiol. 2013; 89:1167–1186. [PubMed: 23869529]

10. Marti M, Good RT, Rug M, Knuepfer E, Cowman AF. Targeting malaria virulence and remodeling proteins to the host erythrocyte. Science. 2004; 306:1930–1933. [PubMed: 15591202]

11. Hiller NL, et al. A host-targeting signal in virulence proteins reveals a secretome in malarial infection. Science. 2004; 306:1934–1937. [PubMed: 15591203]

12. Russo I, et al. Plasmepsin V licenses Plasmodium proteins for export into the host erythrocyte. Nature. 2010; 463:632–636. [PubMed: 20130644]

13. Boddey JA, et al. An aspartyl protease directs malaria effector proteins to the host cell. Nature. 2010; 463:627–631. [PubMed: 20130643]

14. Rock EP, et al. Comparative analysis of the Plasmodium falciparum histidine-rich proteins HRP-I, HRP-II and HRP-III in malaria parasites of diverse origin. Parasitology. 1987; 95 (Pt 2):209–227. [PubMed: 3320887]

15. Spielmann T, et al. A cluster of ring stage-specific genes linked to a locus implicated in cytoadherence in Plasmodium falciparum codes for PEXEL-negative and PEXEL-positive proteins exported into the host cell. Mol Biol Cell. 2006; 17:3613–3624. [PubMed: 16760427]

16. Crabb BS, et al. Targeted gene disruption shows that knobs enable malaria-infected red cells to cytoadhere under physiological shear stress. Cell. 1997; 89:287–296. [PubMed: 9108483]

17. Culvenor JG, Day KP, Anders RF. Plasmodium falciparum ring-infected erythrocyte surface antigen is released from merozoite dense granules after erythrocyte invasion. Infect Immun. 1991; 59:1183–1187. [PubMed: 1997422]

18. Boddey JA, et al. Role of plasmepsin V in export of diverse protein families from the Plasmodium falciparum exportome. Traffic. 2013; 14:532–550. [PubMed: 23387285]

19. Gruring C, et al. Uncovering common principles in protein export of malaria parasites. Cell Host Microbe. 2012; 12:717–729. [PubMed: 23159060]

20. Mundwiler-Pachlatko E, Beck HP. Maurer's clefts, the enigma of Plasmodium falciparum. Proc Natl Acad Sci U S A. 2013; 110:19987–19994. [PubMed: 24284172]

21. Blisnick T, et al. Pfsbp1, a Maurer's cleft Plasmodium falciparum protein, is associated with the erythrocyte skeleton. Mol Biochem Parasitol. 2000; 111:107–121. [PubMed: 11087921]

22. Heiber A, et al. Identification of New PNEPs Indicates a Substantial Non-PEXEL Exportome and Underpins Common Features in Plasmodium falciparum Protein Export. PLoS Pathog. 2013; 9:e1003546. [PubMed: 23950716]

23. Miller LH, Baruch DI, Marsh K, Doumbo OK. The pathogenic basis of malaria. Nature. 2002; 415:673–679. [PubMed: 11832955]

24. Kulzer S, et al. Parasite-encoded Hsp40 proteins define novel mobile structures in the cytosol of the P. falciparum-infected erythrocyte. Cell Microbiol. 2010; 12:1398–1420. [PubMed: 20482550]

25. Klemba M, Beatty W, Gluzman I, Goldberg DE. Trafficking of plasmepsin II to the food vacuole of the malaria parasite Plasmodium falciparum. J Cell Biol. 2004; 164:47–56. [PubMed: 14709539]

26. Yeoh S, et al. Subcellular discharge of a serine protease mediates release of invasive malaria parasites from host erythrocytes. Cell. 2007; 131:1072–1083. [PubMed: 18083098]

27. Morahan BJ, et al. Functional analysis of the exported type IV HSP40 protein PfGECO in Plasmodium falciparum gametocytes. Eukaryot Cell. 2011; 10:1492–1503. [PubMed: 21965515]

28. Nguitragool W, et al. Malaria parasite clag3 genes determine channel-mediated nutrient uptake by infected red blood cells. Cell. 2011; 145:665–677. [PubMed: 21620134]

29. Besteiro S, Michelin A, Poncet J, Dubremetz JF, Lebrun M. Export of a Toxoplasma gondii rhoptry neck protein complex at the host cell membrane to form the moving junction during invasion. PLoS Pathog. 2009; 5:e1000309. [PubMed: 19247437]

30. Jackson KE, et al. Selective permeabilization of the host cell membrane of Plasmodium falciparum-infected red blood cells with streptolysin O and equinatoxin II. Biochem J. 2007; 403:167–175. [PubMed: 17155936]

31. Liu J, Gluzman IY, Drew ME, Goldberg DE. The role of Plasmodium falciparum food vacuole plasmepsins. J Biol Chem. 2005; 280:1432–1437. [PubMed: 15513918]

32. Balu B, Shoue DA, Fraser MJ Jr, Adams JH. High-efficiency transformation of Plasmodium falciparum by the lepidopteran transposable element piggyBac. Proc Natl Acad Sci U S A. 2005; 102:16391–16396. [PubMed: 16260745]

33. Hall R, et al. Antigens of the erythrocytes stages of the human malaria parasite Plasmodium falciparum detected by monoclonal antibodies. Mol Biochem Parasitol. 1983; 7:247–265. [PubMed: 6350871]

34. Anders, RF.; NB; Shi, PT.; Scanlon, DB.; Brown, LE.; Thomas, LM.; Brown, GV.; Stahl, HD.; Coppel, RL.; Kemp, DJ. Molecular Strategies of Parasitic Invasion. Goodman, H.; Agabian, N.; Noguiera, N., editors. Alan R. Liss; 1987. p. 333-342.

35. Kumar N, Koski G, Harada M, Aikawa M, Zheng H. Induction and localization of Plasmodium falciparum stress proteins related to the heat shock protein 70 family. Mol Biochem Parasitol. 1991; 48:47–58. [PubMed: 1779989]

36. Hawthorne PL, et al. A novel Plasmodium falciparum ring stage protein, REX, is located in Maurer's clefts. Mol Biochem Parasitol. 2004; 136:181–189. [PubMed: 15481109]

37. Eksi S, et al. Identification of a subtelomeric gene family expressed during the asexual-sexual stage transition in Plasmodium falciparum. Mol Biochem Parasitol. 2005; 143:90–99. [PubMed: 15996767]

38. Frankland S, et al. Serum lipoproteins promote efficient presentation of the malaria virulence protein PfEMP1 at the erythrocyte surface. Eukaryot Cell. 2007; 6:1584–1594. [PubMed: 17644656]

39. Francis SE, Banerjee R, Goldberg DE. Biosynthesis and maturation of the malaria aspartic hemoglobinases plasmepsins I and II. J Biol Chem. 1997; 272:14961–14968. [PubMed: 9169469]

40. Ragge K, et al. In vitro biosynthesis and membrane translocation of the serine rich protein of Plasmodium falciparum. Mol Biochem Parasitol. 1990; 42:93–100. [PubMed: 2122249]

41. Gruring C, Spielmann T. Imaging of live malaria blood stage parasites. Methods Enzymol. 2012; 506:81–92. [PubMed: 22341220]

42. Ginsburg H, Kutner S, Krugliak M, Cabantchik ZI. Characterization of permeation pathways appearing in the host membrane of Plasmodium falciparum infected red blood cells. Mol Biochem Parasitol. 1985; 14:313–322. [PubMed: 3887158]

43. Kirk K, Horner HA, Elford BC, Ellory JC, Newbold CI. Transport of diverse substrates into malaria-infected erythrocytes via a pathway showing functional characteristics of a chloride channel. J Biol Chem. 1994; 269:3339–3347. [PubMed: 8106373]

44. Babbitt SE, et al. Plasmodium falciparum responds to amino acid starvation by entering into a hibernatory state. Proc Natl Acad Sci U S A. 2012; 109:E3278–3287. [PubMed: 23112171]
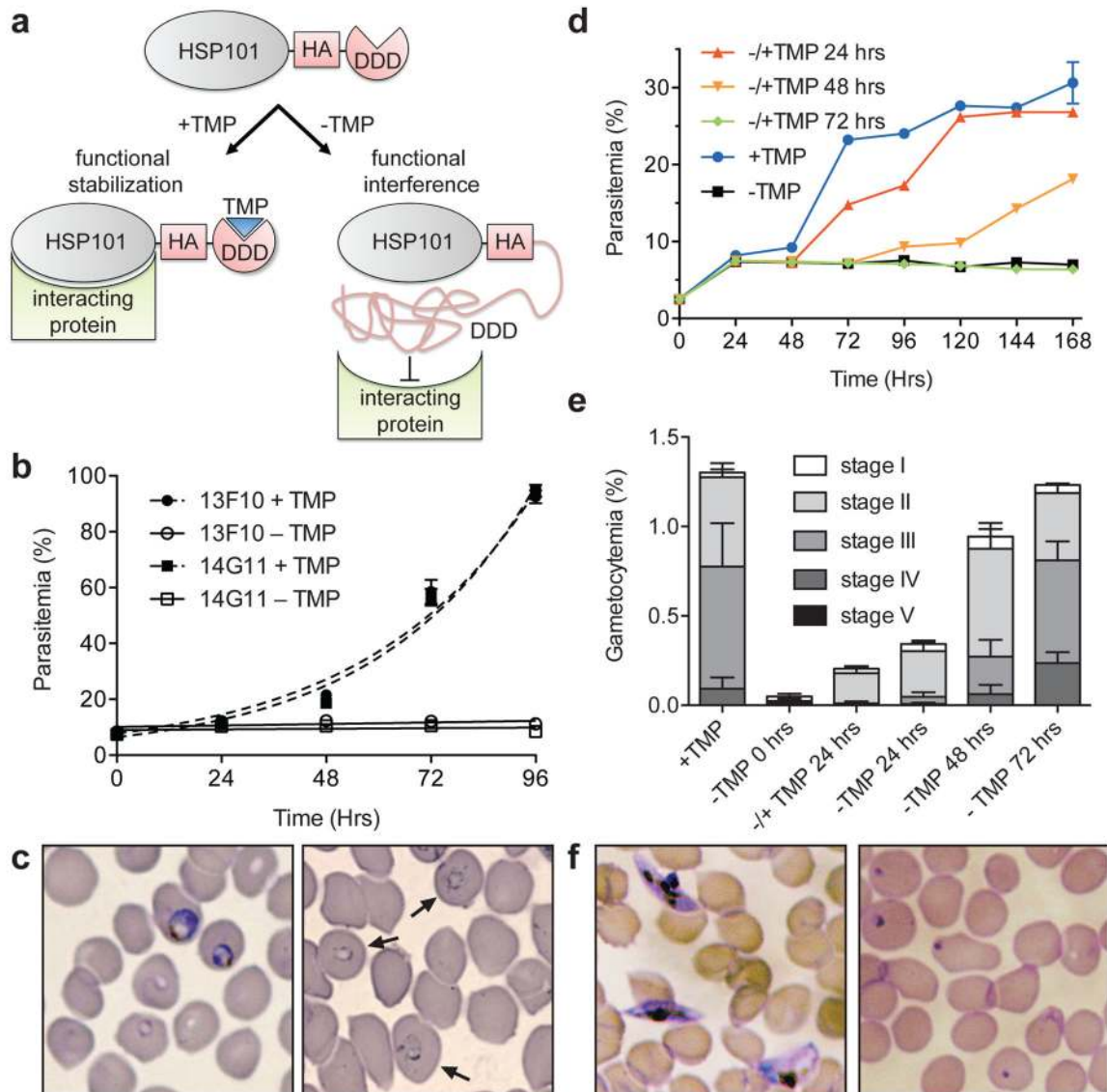
Figure 1. HSP101 is essential for development of asexual and sexual blood stages
a, Auto-inhibition strategy for HSP101^{DDD}. TMP, trimethoprim; HA, hemagglutinin tag; DDD, DHFR destabilization domain. **b,** Growth analysis of asynchronous cultures of the two independent clones 13F10 and 14G11 +/− TMP. Error bars represent s. d. of three technical replicates. Data are representative of three independent experiments. **c,** Giemsa-stained smears of cultures following 48 hours +/− TMP. Accumulation of late ring stage parasites is observed in the absence of TMP (arrows). Images are representative of three independent experiments. **d,** Growth analysis of synchronous 13F10 parasites. TMP was removed at the early trophozoite stage and added back to cultures after 24, 48 or 72 hours. Equivalent parasitemia in all samples at 24 hours shows that development through trophozoite and schizont stages, egress and reinvasion were not affected by TMP removal. Error bars as in **b**. Data are representative of three independent experiments. **e,** Analysis of gametocyte formation by 13F10 parasites. TMP was removed from late schizonts following

gametocyte induction (0 hrs) or at subsequent 24 hour intervals. In one sample, TMP was removed at 0 hours and restored after 24 hours (−/+ TMP 24 hrs). Gametocytemia of various stages on day nine post-induction is shown. Error bars as in **b**. Data are representative of four independent experiments. **f,** Giemsa-stained smears of gametocyte cultures nine days post induction. Images are representative of four independent experiments.
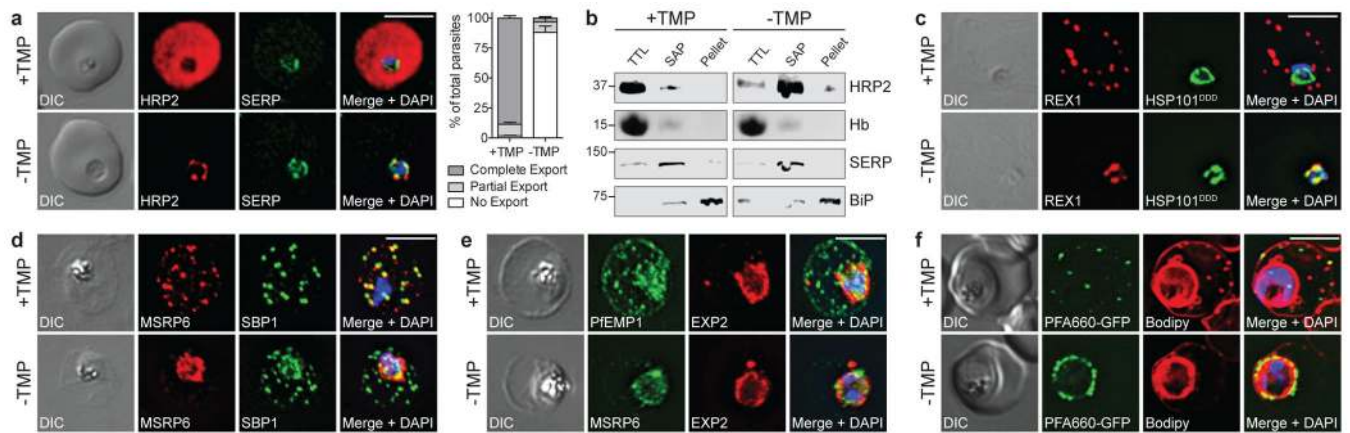
Figure 2. HSP101 is required for export of PEXEL and PNEP proteins

a, c IFA of ring-stage 13F10 parasites +/− TMP. TMP was removed in late schizont stage and parasites were allowed to reinvade and grow 18–24 hours before fixation with paraformaldehyde (a) or acetone (c). **a,** IFA of the exported PEXEL-containing protein HRP2. SERP is a marker for the PV. Export was scored as complete (no HRP2 signal enrichment around the parasite as shown in the +TMP IFA), partial (HRP2 signal within the host cell but also enriched around the parasite) or no export (HRP2 signal only seen around the parasite and not in the host cell, as shown in the −TMP IFA). Error bars represent s. d. of three technical replicates. Data are representative of five independent experiments. **b,** Sequential fractionation of infected ring-stage parasites +/− TMP analyzed by Western blot. The host cytosol was released with tetanolysin (TTL) and subsequently the PV contents were released with saponin (SAP). Blocked HRP2 is found in the PV fraction. Hemoglobin (Hb) was detected by Coomassie staining and serves as a control for host cytosol release. SERP serves as a control for PV release. BiP serves as a parasite integrity control. Data are representative of two independent experiments. **c,** IFAs of the PNEP REX1, which colocalizes with HSP101^{DDD} at the PVM in the absence of TMP. **d, e** IFA of trophozoite-stage 13F10 parasites +/− TMP. TMP was removed in late ring stage and parasites were allowed to develop 12–24 hours before fixation with acetone. **f,** Live fluorescence imaging of 13F10 parasites expressing a PFA660-GFP fusion and labeled with Bodipy TR Ceramide to demarcate the PVM (other membranes are also labeled). TMP treatment as in **d, e**. All scale bars = 5μm. Images in **c–f** are representative of two independent experiments.
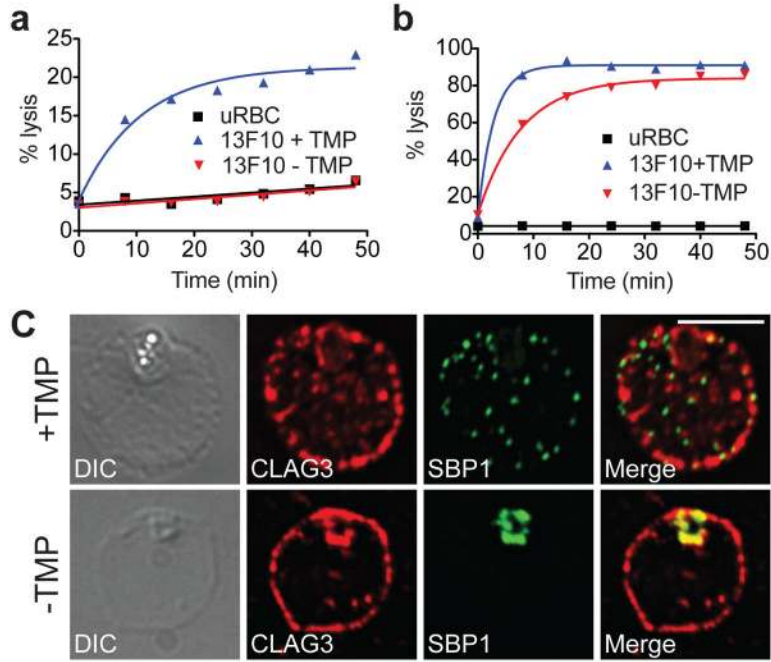
Figure 3. HSP101 is required for activation of PSAC but not trafficking of CLAG3 to the RBC periphery

a, b Osmotic lysis assay on 13F10 parasites. Sorbitol-sensitivity of arrested, late ring stage (−TMP) and control (+TMP) parasites at 25% parasitemia (a) or later stages +/− TMP magnet-purified to >95% parasitemia (b) is shown. Error bars represent s. d. of three technical replicates. Results are representative of two independent experiments. **c,** IFA of ring stage 13F10 parasites showing CLAG3 localization to the RBC membrane +/− TMP. TMP was removed in the late schizont stage and parasites were allowed to develop 18 hours before fixation with 90% acetone/10% methanol. Scale bar = 5μm. Images are representative of two independent experiments.
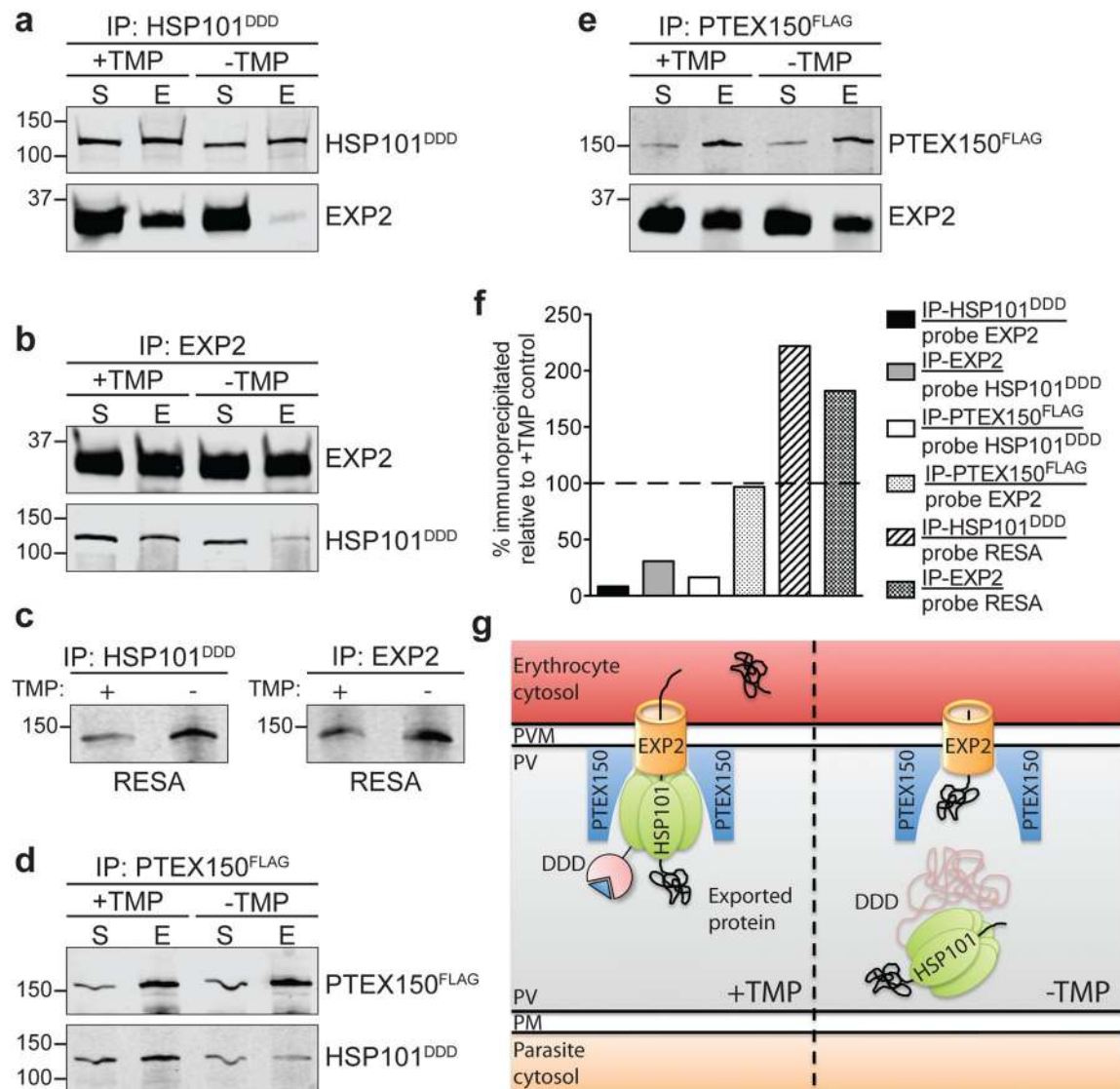
Figure 4. Inactivated HSP101^{DDD} dissociates from the PTEX complex
a–c, Immunoprecipitation (IP) of PTEX components from lysates of 13F10 parasites. S, supernatant input. E, elution. **d, e,** IP of PTEX components from lysates of 13F10 parasites expressing a PTEX150-FLAG fusion protein. **f,** Quantification of IP data. Data are representative of three independent experiments. **g,** Model for mechanism of export block following inactivation of HSP101^{DDD}. HSP101 recognizes exported substrates and drives their translocation across the PVM in conjunction with other PTEX components by unfolding and/or directional threading. Destabilization of the DDD tag results in dissociation of HSP101 from PTEX, blocking translocation. Continued interaction of HSP101^{DDD} and EXP2 with exported substrates in these conditions suggests substrate molecules may be trapped at various steps in the translocation process.